

# **EFFECT OF THERMAL CYCLING THROUGH PHASE TRANSFORMATIONS ON MICROSTRUCTURAL BANDING AND DIFFUSION IN STEELS**

**A Thesis Submitted  
in Partial Fulfilment of the Requirements  
for the Degree of  
MASTER OF TECHNOLOGY**

*by*

**By  
JITENDRA SINGH**

*to the*

**DEPARTMENT OF METALLURGICAL ENGINEERING  
INDIAN INSTITUTE OF TECHNOLOGY, KANPUR  
March, 1989**

**CERTIFICATE**

Certified that this work entitled "Effect of the Thermal Cycling Through Phase Transformations on Microstructural Banding and Diffusion in Steels" submitted by Jitendra Singh has been carried out under my supervision and the same has not been submitted elsewhere for a degree.



**DR. ROMESH C. SHARMA**  
Professor

Department of Metallurgical Engineering  
Indian Institute of Technology  
Kanpur.

Th

669.14E

Si 64c

CENTRAL LIBRARY

Acc. No. 105933

ME-1989-M-SIN-EFF

**ACKNOWLEDGEMENTS**

I would like to express my deep sense of gratitude and indebtedness to my guide Dr. Romesh C. Sharma, Professor, Department of Metallurgical Engineering for his guidance and supervision. I consider it my privilege to have the golden opportunity to work under him. I have no hesitation in declaring that without his constant help and encouragement, this work would not have been possible.

I am grateful to Mr. M.N. Mungale, Mr. C.L. Sachan, Mr. K.P. Mukharjee & Mr. H.C. Shrivastava staff members in Metallurgical Engineering Department for their help at various stages of this project work.

I am ever indebted to my friends; Mr. D.Bhattacharyaji, Mr. A.Ranjan, Mr. N.Joshi, Mr. V.Bhusan, Mr. S.R. Ponkshe, Mr. I.Mukherjee, Mr. S.Singh for their cooperation and support.

The generous help of Mr. O.P. Pandey in excellent typing of the manuscript is gratefully acknowledged.

**(JITENDRA SINGH)**

ABSTRACT

Microstructural ferrite-pearlite banding which occurs in commercial steels has been simulated by means of diffusion layer couples. Effect of thermal-cycling treatment between 600 and 950°C at constant heating and cooling rates of 10°C/min. on microstructural banding and diffusion characteristics of alloying elements has been investigated. Micro-structural banding was substantially reduced after thermal cycling for 200 cycles. Thermal cycling results in marked grain refinement and better distribution of phases. Qualitative (Mn-profile and microstructural) analysis has indicated that diffusion mobility of substitutional alloying element (Manganese) was more during thermal cycling treatment as compared to annealing. The possible reasons have been discussed.

## CONTENTS

Chapter	Page No.
CERTIFICATE	- I -
ACKNOWLEDGEMENT	-II- -
ABSTRACT	-III-
LIST OF TABLES	-IV-
LIST OF FIGURES	- V-
1. INTRODUCTION	1
2. LITERATURE REVIEW	3
2.1 Microstructural Banding	3
2.2 Kinetic Factors in Banding	4
2.3 Effect of Microstructural Banding on Mechanical Properties of Steel	5
2.3.1 Tensile Properties	6
2.3.2 Notch Impact Properties	6
2.3.3 Fatigue Crack Propagation	7
2.4 Effect of Banding on Welding Behaviour	7
2.5 Effect of Banding on the Machinability	8
2.6 Effect of Banding on Austenite Transformation	8
2.7 Elimination of Banding	10
2.8 Effect of Alloying Elements on The Rate of Diffusion Controlled Transformation in Steel	13
2.8.1 Manganese Partitioning During The Austenite to Proeutectoid Ferrite Transformation	14
2.8.2 Manganese Partitioning During The Austenite-Pearlite Transformation	15
2.8.3 Kinetics of Austenite Formation in Steel with Ferrite-Pearlite Microstructure	17

Chapter		Page No.
2.9	Thermal Cycling Treatment	24
2.9.1	General	24
2.9.2	Features of $\alpha$ - $\gamma$ Transformation in Engineering Steels Subjected to Thermal Cycling	24
2.9.3	Transformation Kinetics of The Austenite of The Engineering Steels During Thermal Cycling Treatment	25
2.9.4	Diffusion During The Thermal Cycling of Steels	30
2.9.5	Effect of Thermal Cycling on Mechanical* of Steels	30
3	EXPERIMENTAL PROCEDURE	32
3.1	Selection of Material	32
3.2	Preparation of Diffusion Couples	32
3.3	Heat Treatment of Diffusion Couple	35
3.3.1	Annealing Treatment	35
3.3.2	Thermal Cycling Treatment	35
3.4	Treatment of Steel With Banded Microstructure	37
3.5	Electron Probe Micro Analysis	39
4	RESULT AND DISCUSSION	40
4.1	Microstructure	40
4.2	Electron Probe Micro Analysis	43
4.3	Discussion	46
5	CONCLUSIONS	51
	REFERENCES	

LIST OF TABLES

Table No.		Page No.
2.1	Kinetic Factors in Commercial Banding	5
3.1	Composition of Base Plates	32
3.2	Annealing Schedule	35
3.3	Thermal Cycling Schedule	37



LIST OF FIGURES

Figure No.	Page No.
2.1 Effect of Banding on Isothermal Transformation of Austenite	9
2.2 Influence of Cooling Rate on Structural Banding in 20 K Steel	12
2.3 730°C isotherm for Iron-rich Alloys in the Fe-C-Mn Alloy Systems. Showing Boundary Between Partition & No-Partition line	16
2.4 Calculated no Partition Phase Boundaries for Steels Containing 0,1, and 2% Mn.	18
2.5 Logarithm of The Partition Coefficients of Manganese Vs Reciprocal of The Absolute Temperature for the 1 % and 2% Mn Steels	19
2.6 Calculated Growth Rates for The 1% Mn Steel Assuming Volume Diffusion or Boundary Diffusion of Carbon as Rate Controlling Mechanisms	20
2.7 Kinetics of Austenite Formation in 0.20 C-1.5 Mn Steel	22
2.8 Schematic Diagrams of Three Steps in Austenite Growth During Intercritical Annealing of Ferrite-Pearlite Steels	23
2.9 Frequency Distribution of Size of Austenite Grains of Steel.	26
2.10 Isothermal Transformation of Austenite of Steel.	28
2.11 Kinetics of Ferrite-Pearlite Transformation of Austenite of Steel	29

Figure No.	Page No.
3.1 The Micrograph of Base Plate of Composition N <sub>2</sub>	33
3.2 The Micrograph of Base Plate of Composition N <sub>15</sub>	33
3.3 The Micrograph of Rolled low C-Mn Steel	33
3.4 The Assembly Used to Make Diffusion Couples	34
3.5 Micrograph of Typical Diffusion Layer Couple Showing Simulated Banding Effect near Welds	36
3.6 Thermal Cycling Schedule used for The Experiment	38
4.1 The Micrograph of Simulated Diffusion Layer Couple I	41
4.2 The Micrograph of Diffusion Couple I Annealed for 6 Days at 950°C	41
4.3 The Micrograph of Diffusion Couple I Thermal Cycled for 100 Cycles	41
4.4 The Micrograph of Simulated Diffusion layer Couple II	42
4.5 The Micrograph of Diffusion Couple II Annealed for 12 Days at 950°C	42
4.6 The Micrograph of Diffusion Couple II Thermal Cycled for 100 Cycles	42
4.7 The Micrograph of Diffusion Couple II Thermal Cycled for 200 Cycles	42
4.8 The Micrograph of Rolled Low C-Mn Steel	44
4.9 The Micrograph of Rolled Low C-Mn Steel Annealed for 6 Days at 950°C	44
4.10 The Micrograph of Rolled Low C-Mn Steel Thermal Cycled for 50 Cycles	44.
4.11 The Micrograph of Rolled Low C-Mn Steel Thermal Cycled for 100 Cycles	44.

Figure No.	Page No.
4.12 The Mn Profile for Simulated Diffusion Layer Couple II	45
4.13 The Mn Profile for Diffusion Couple II Annealed for 12 Days at 950°C	45
4.14 The Mn-Profile for Diffusion Couple II Thermal Cycled for 100 Cycles	45
4.15 The Mn-Profile for Diffusion Couple II Thermal Cycled for 200 Cycles	45
4.16 Schematic Representaion of the Evolution of the Activity Surface on an Fe-C-Mn Diffusion Layer Couple	48

## CHAPTER - 1

### INTRODUCTION

Microstructural banding, particularly ferrite-pearlite banding is a common defect in low carbon steels. The banding phenomena has been the subject of numerous investigation. Although other factors have been considered, it is generally agreed that the primary cause of micro-structural banding is the segregation of one or more elements. The segregation arises during solidification as a result of substantial temperature difference between the solidus and liquidus. Other factors influence the degree, type and form of banding by their influence on the degree of chemical segregation. Some of these factors are austenization temperature and time, diffusion rates of carbon and alloy, grain size, cooling rate and rates of nucleation and growth of decomposition product of austenite.

Microstructural banding results in marked anisotropy in mechanical properties, causes difficulty in welding by promoting different transformation reaction in areas of varying carbon content. In steels whose chemical composition leads to severe dendritic segregation in the ingot and hence to severe banding in product, bands of martensite may be present in an otherwise relatively soft matrix microstructure. After certain heat treatments such hard band may lead to difficulty in machining and cold forming. And therefore microstructural banding causes rejection of such steels for various uses.

Complete and permanent removal of microstructural banding is, in most steel products, beyond the range of economic feasibility. Insofar as microstructural banding is concerned but not in respect to elimination of alloy concentration gradient, can be achieved by simply heating for 10 minutes at 1315°C and air cooling. But it reappears on subsequent rolling[1]. However, accelerated cooling schedules have been developed to eliminate or minimise this phenomena economically. Two such schedules developed by Gul et. al[2] were adopted for elimination of banded structure in boiler tubes at Nikopol

Southern Tube Works, U.S.S.R., with a resultant annual saving of 35000 roubles.

Thermal cycling treatment is known to be used for grain refinement, removing defects, intensifying chemicothermal treatment and improving cold formability. The wider use of thermal cycling treatment in industrial production is, however hindered by the absence of theoretical developments regarding the structural and phase transformations during this type of processing which in the final analysis, determine the properties of material.

In present investigation microstructural banding has been simulated by means of diffusion layer couples, constructed of high purity iron based alloys. Efforts have been made to determine the effect of thermal cycling treatment between 600 and 950°C at constant heating and cooling rates of 10°C/min. on ferrite pearlite banded structure with the help of stimulated diffusion couples and as-rolled specimens of lowC-Mn steel containing banded structure. Emphasis has been laid mainly on the structural and phase transformations and diffusion characteristics of alloying elements during thermal cycling treatment. The effect of thermal cycling treatment on microstructural banding has also been compared with the effect of annealing treatment on the same.

## CHAPTER - 2

### LITERATURE REVIEW

#### 2.1 Microstructural Banding :

The appearance of alternate ferrite-pearlite bands in rolled and forged hypoeutectoid steel products is primarily associated with persistent segregation of alloying elements other than carbon. This segregation originates in normal interdendritic segregation during solidification of ingot and, because of slow diffusion of many elements (particularly substitutional ones) at working and soaking temperatures, it persists in a more or less moderate form into the final product in laminar distribution. [3].

Other factors influence the degree, type and form of banding by their influence on the degree of chemical segregation, some of these factors are austenizing temperature and time, diffusion rates of carbon and alloying elements, grain size, cooling rate and rates of nucleation and growth of decomposition products of austenite.

Jatezak et. al.[4] have studied the effect of various factors in detail and their results can be expressed as follows :

1. Primary cause of banding in rolled steel products is chemical heterogeneity. The effect of other nucleating agents such as banded inclusions etc. are either minor or non existent.
2. Chemical heterogeneity produces visible banding through its effect on nucleation and growth of ferrite and pearlite from austenite. The pattern of nucleation and growth of ferrite and pearlite is determined primarily by the aggregate effect of heterogeneity on carbon segregation.
3. In the analysis studied carbide forming elements tend to increase carbon concentration in their vicinity, while solution forming elements (Nickel) tend to decrease carbon concentration in their vicinity. Therefore in single alloyed steels the degree of carbon segregation and location of high and low carbon areas relative to a fixed

marker depend solely on the amount and distribution of one alloying element. As noted in the paper, the location of high carbon bands relative to inclusions differs for the carbide forming elements versus nickel. In multialloy steels these visual banded conditions depend upon a balanced influence as determined by alloy type, amount and distribution.

4. The overall effect of chemical heterogeneity on nucleation and growth of ferrite and pearlite from austenite into carbon segregated structure is influenced by the added effect of cooling conditions from austenizing temperature and also transformation.

A relatively low cooling rate ( $3-5^{\circ}\text{C}/\text{sec}$ ) also promotes structural banding. In this case diffusional decomposition of austenite starts with low degree of supercooling (about  $50^{\circ}\text{C}$ ) beyond  $A_{r3}$  which ensures the preferential influence of chemical microheterogeneity in the austenite on the nucleation process. [2].

## 2.2 Kinetic Factors in Banding :

In evaluating the degree to which certain elements are responsible for banding in steel one must determine the extent to which each element is segregated on initial solidification of the melt and the rate at which segregation will be reduced by diffusion. Table 2.1 has been constructed giving estimates of the segregation coefficients [5],[6],[7] ( $1-K$ , where  $K$  is the distribution coefficients obtained from the phase diagram) and a typical austenitic diffusion coefficient for several elements of interest [8]. Qualitatively, we may presume that large segregation coefficients and low diffusion coefficients will favour banding.

TABLE 2.1

**Kinetic factors in Commercial banding**

Alloy Addition	Segregation Coefficient 1-K for $\delta$ -Iron	Diffusion Coeff. (Cm <sup>2</sup> /sec)	
		1000°C	1200°C
Silicon	0.16	$7.5 \times 10^{-9}$	$1.4 \times 10^{-8}$
Manganese	0.87	$4.1 \times 10^{-10}$	$5.8 \times 10^{-9}$
Nickel	0.42	$2.4 \times 10^{-12}$	$9.0 \times 10^{-11}$
Chromium	0.15	$7 \times 10^{-11}$	$1.0 \times 10^{-9}$
Phosphorus	0.71	$1 \times 10^{-10}$	$5 \times 10^{-9}$

**2.3 Effect of Microstructural Banding on Mechanical Properties of Steel**

A study by Grang [1] has shown that high temperature normalizing treatment was capable of removing pearlite-ferrite banding in a 0.25 pct carbon 1.5 pct Mn Steel which made it possible to compare mechanical properties in specimens that differed only in pearlite banding. Although the normalizing treatment removed pearlite banding, it did not completely remove the pattern of alloy microsegregation in the steel. Because of the short time of the high temperature normalizing treatment, inclusion morphology was assumed to be the same in banded and unbanded specimens.

Using above concept, spitzig [9] has studied the deleterious effect of inclusions and pearlite banding on anisotropy of tensile ductility and notch toughness in a series of hot rolled 0.2 pct carbon, 1.0 pct manganese steel specimens containing either 0.004 or 0.013 pct sulphur with and without rare-earth additions by giving a short time high temperature normalizing treatment for removal of pearlite banding and then normalizing a second time, but at lower temperature to reduce the grain size, after which they were compared with specimens which recieved only the lower temperature normalizing treatment and reached to following conclusion.



### 2.3.1 Tensile Properties :

There were no obvious difference between the strain curves for the steels in banded and nonbanded conditions. Data shows no significant difference in the yield and tensile strength values between the banded and non banded conditions for a given steel. However, the total elongation, fracture strain and reduction of area of the through thickness specimens of steel containing stringered sulphide inclusions were considerably improved after removal of pearlite banding.

When the sulphide inclusions were globular or the sulfur content was very low, the removal of banding had no apparent effect on through thickness properties. This suggests that pearlite banding is detrimental to tensile ductility only when stringered sulphide inclusions are also present, however this is a result of inclusion being more globular in the nonbanded steel.

### 2.3.2 Notch Impact Properties :

The temperature for 50 percent brittle fracture often referred to as fracture transition temperature (F.T.T), is used frequently as a criterion for relative toughness. FTT is not significantly changed by banding, inclusions, nor specimen orientation ; although the energy absorbed at the FTT is affected by these factors. In the ferrite pearlite microstructure FTT is  $-4^{\circ}\text{C}$  and in the tempered martensite it is  $-73^{\circ}\text{C}$  indicating that FTT in this particular steel is principally influenced by microstructure.

The effect of banding, inclusions and specimen orientation on fracture energy varies with the proportion of ductile and brittle fracture. Energy for brittle fracture for a specimen with banding is always higher than corresponding unbanded specimen thus banding decreases self energy.

### 2.3.3 Fatigue Crack Propagation

Studies were made on the effect of dendritic heterogeneity on the contact fatigue damage of rails. Fatigue crack development occurred mainly at the areas of banded structure and not at non-metallic inclusions of oxide or sulphide type. Diffusion anneal is recommended to reduce the effect of banded structure [10].

The E 37 steel contained 0.14 pct carbon, 1.32 pct Mn, 0.47 pct Si, 0.040 pct Ni and was in the form of hot rolled plates 86 mm thick, compact tension test pieces 25 mm thick and 3.12 mm wide, 27.5 mm deep transverse notch in one side, were taken at various angle of 0 to 90° to the plane of rolling and tested at a frequency of 20 Hz. the result shows that speed of crack propagation is maximum when parallel to this direction of rolling and minimum at 45° to this but the difference is at the most four times. The different speeds can be explained by the tendency of secondary cracking to take place at the intermediate angle. [11].

### 2.4 Effect of Banding on Welding Behaviour :

In spite of a controlled carbon equivalent and normal welding precautions, cracks were noted in the heat effected zone in 20 mm plates of welded construction steel. Metallographic examinations revealed a heavily banded structure of pearlite rich and ferrite rich areas. Experimental work was conducted to find out the behaviour of these striations on heating above the critical temperature and also on quenching. Results indicate that the welding process prompts a different transformation reaction between areas of varying carbon content. This causes the material to behave as a high carbon steel and cause welding difficulties associated with this type of material [12].

## 2.5 Effect of Banding on the Machinability :

The effect of pearlite banding on the machinability of AISI 12 L 14 leaded low carbon resulphurised steel was investigated, the results obtained can be summarized as follows. Surface finish observed in the plung test improves with increasing continuity and interval of pearlite banding. The effect of pearlite banding was not observed on drill life. The improved surface finish has been attributed to more stable formation of built up edges and to the reduction in groove wear length. The severity of pearlite banding in low carbon resulphurised free machining steels depends on the change in  $A_{r3}$  temperature due to microsegregation of phosphorus and manganese and on cooling rate after rolling. The optimum pearlite structure for machinability could be obtained by reheating at low temperature for short time before rolling and slow cooling after rolling [13].

## 2.6 Effect of Banding on Austenite Transformation :

Effect of microstructural banding on transformation of austenite has been studied by Grang [1] at various temperatures. Results are summarized in Fig 2.1. At all temperatures, transformation began slightly sooner in the steel without banding. However below  $650^{\circ}\text{C}$ , its transformation was completed in slightly shorter time. Overall the effect of banding on austenite transformation is comparatively small. Davenport [14] found that in a 0.35 percent carbon, 1.85 percent manganese steel, when banding was removed by a homogenization treatment of 48 hours at  $1250^{\circ}\text{C}$ , the beginning of transformation was slightly retarded and completion accelerated. He also observed that above about  $595^{\circ}\text{C}$  this overall trend was reversed and completion was retarded in the steel without banding.

Fig. 2.1 shows that transformation kinetics are not altered to

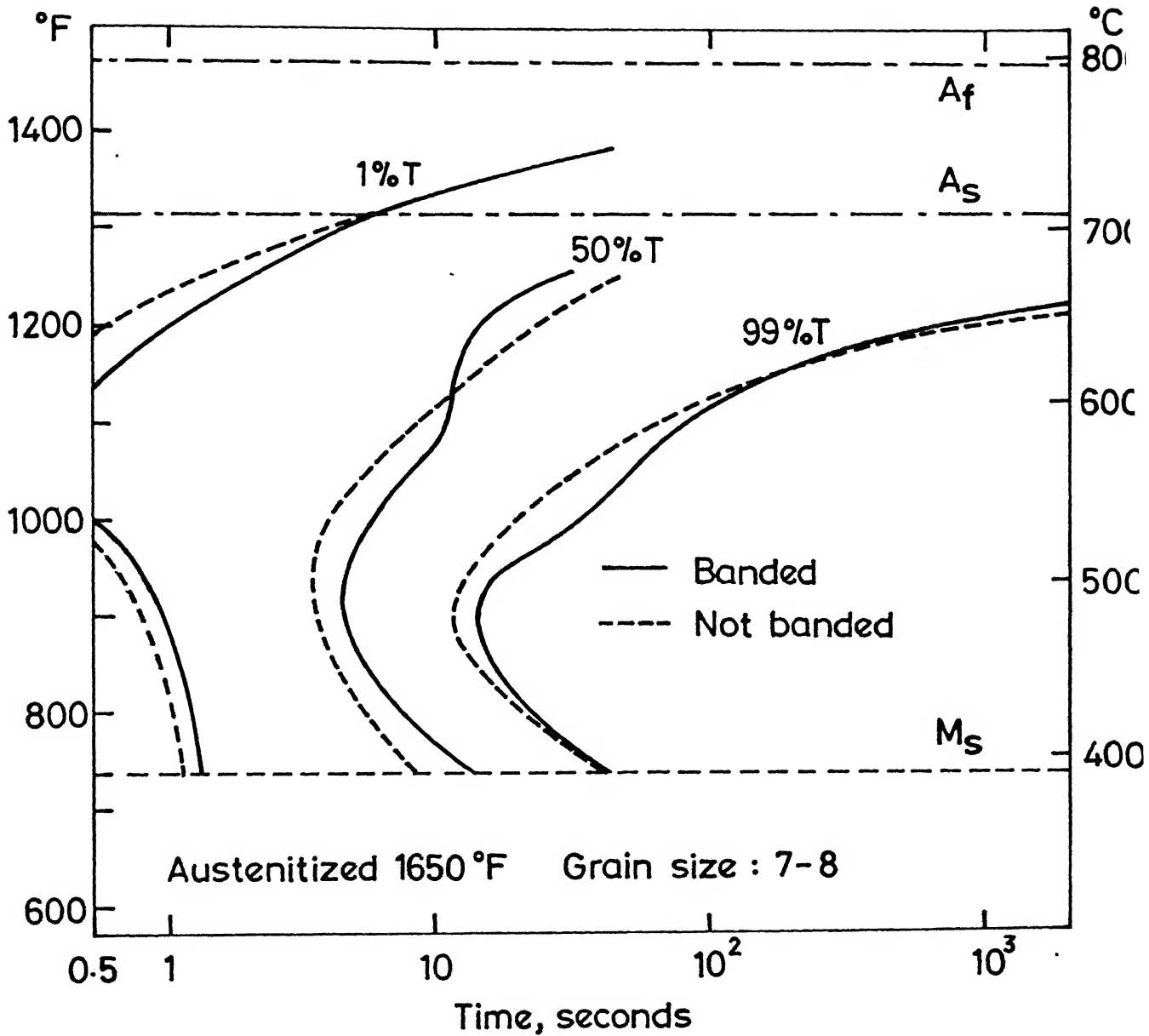


Fig. 2.1 Effect of banding on isothermal transformation of austenite.

any great extent by removal of banding. A small decrease in hardenability is indicated by the isothermal transformation, and this was confirmed independently by hardenability tests. Any decrease in transformation time by removal of banding is of minor consequence. The important feature is that a few percent of untransformed martensite in banded steel is concentrated in relatively few bands, where-as when banding is removed, essentially the same amount of martensite will be present as randomly dispersed small particles. The latter almost certainly are the most desirable in respect to machinability and cold forming.

## 2.7 Elimination of Banding :

Complete and permanent removal of microstructural banding by homogenization is, in most steel products beyond the range of economic feasibility.

The demonstration that constitutional effects are dominant in the production of banding allows one to construct a formula for estimating the cooling rates,  $\dot{T}$  necessary for suppression of intense banding in terms of the constitutional temperature difference  $\Delta T$  between layers, the mean carbon diffusion constant  $D$  within this temperature range, and mean segregated spacing,  $W$ .  $\dot{T} > 5 D \Delta T / W^2$  [15].

This is obtained by equating the spacing to the diffusion length corresponding to time in the range  $\Delta T$  and multiplying  $\dot{T}$  by a marginal factor of 5.

The steel with C=0.25 percent, Mn=1.5 percent heat treated to remove microstructural banding by heating for 10 minutes at 1315°C to 1345°C and then air cooling. Banding in steel was removed by this high temperature normalizing treatment. The reason for the effectiveness of

of the short time high-temperature normalizing in removing microstructural banding is not well understood. It does do so, as these results demonstrate, to the extent that subsequent treatments, such as annealing, normalizing or hardening may be done repeatedly or in combination without return of banding. However, if steel in which banding has been eliminated by high temperature normalizing is subsequently hot rolled or otherwise deformed and then reaustenized, banding returns to progressively greater\* as the amount of deformation is greater. Hence the pattern of alloy segregation responsible for banding must remain and is altered to only a minor degree by the high temperature normalizing treatment. This of course, is what to be expected, since 10 minute is for too short a time for substantial diffusion of substitutional elements [1].

The influence of cooling rate on structure and properties of tubes of 20K steel (composition C 0.20 pct, Mn 0.60 pct, Si 0.25 pct) was studied by varying cooling rates between 0.05 and 200<sup>0</sup>C/sec. Structural banding was found to be removed by cooling at a rate of 50-100<sup>0</sup>C/sec to room temperature (see fig 2.2). But steel properties in this instance were below the specifications for boiler tubes. Trials with interrupted cooling to 600-650<sup>0</sup>C at a rate of 100<sup>0</sup>C/sec enabled a homogeneous structure to be obtained, together with the desired boiler quality. Accelerated interrupted cooling can be used for reliable elimination of structural banding in boiler tubes by treatment after special heating. This treatment is, however, difficult to arrange in line in the continuous mill with a tube rolling speed of upto 10m/sec [2].

Another way of eliminating banded structure involved the formation in the austenite of a large number of uniformly dispersed sites for preferential

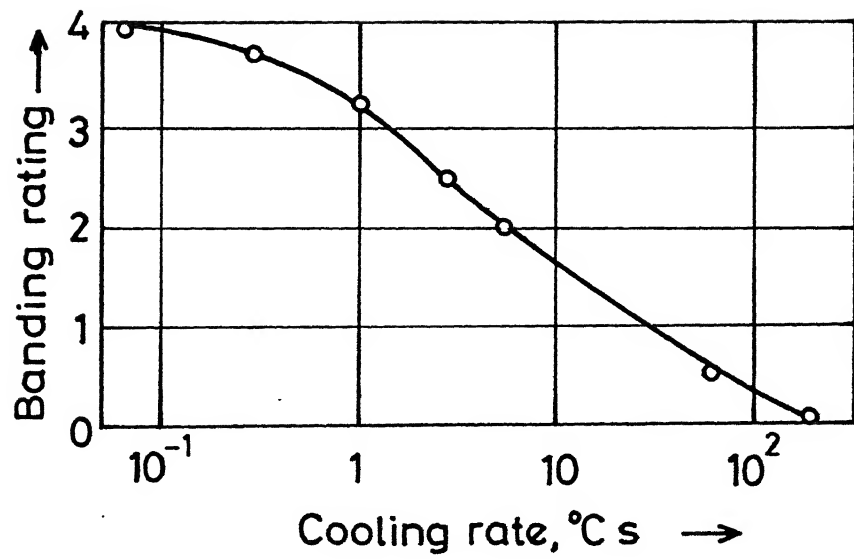


Fig.2.2 Influence of cooling rate on structural banding in 20 K steel [2].

heterogeneous nucleation by special pulsed cooling of the tube surface at rates in excess of  $200^{\circ}\text{C}/\text{sec}$  to  $600\text{--}650^{\circ}\text{C}$  while retaining the matrix in the austenite condition [16]. This eliminates the preferential influence of chemical heterogeneity and non-metallic inclusions on nucleation so that austenite decomposition occurs uniformly throughout the tube, eliminating or minimising structural banding.

## 2.8 Effect of Alloying Elements on the Rate of Diffusion Controlled Transformations in Steel:

Most substitutional alloying elements retard the rate of diffusion controlled transformation in steel. The alloying effect on growth may be attributed to three factors.

1. The effect of alloying element on the Fe-C phase diagram.
2. Ternary diffusion interactions.
3. Diffusion 'drag' due to slowly diffusing alloying element.

The basic influence of substitutional alloying\* <sup>element</sup> 'x' upon the growth kinetics of proeutectoid ferrite in Fe-C-X alloys is exerted through the long recognized thermodynamic effect of the displacement of the equilibrium or paraequilibrium  $\text{Ae}_3$  ( $\gamma/\alpha+\gamma$ ) phase boundary relative to the  $\text{Ae}_3$  curve for Fe-C alloys. This change alters the driving force for the growth of ferrite. Within this thermodynamic framework, two kinetic effects upon ferrite growth kinetics have also been recognized. One is solute drag like effect, where segregation of x to mobile  $\alpha:\gamma$  boundaries changes the activity of the carbon in austenite in immediate contact with these boundaries and hence alters their migration kinetics. The second kinetic effect is exerted by carbide precipitation in association with stationary  $\alpha:\gamma$  boundaries. Such precipitation can either increase or decrease the driving force acting



on adjacent mobile areas of these boundaries. At the present time, the solute drag like effect appears the more important, to the point where it can overbalance the thermodynamic effect when both the bulk concentration of x and the binding energy of 'x' to mobile  $\delta/\gamma$  boundaries are large [17].

Effect of manganese on the austenite to proeutectoid ferrite transformation and austenite to pearlite transformation in Fe-C-Mn system has been discussed in detail in following sections.

#### 2.8.1 Manganese Partitioning During the Austenite to Proeutectoid Ferrite Transformation :

Since manganese depresses the  $A_{e3}$  line, we may expect that this will produce a strong retarding effect at a given temperature due to constitutional effects alone. Furthermore, since the proeutectoid reaction involves rejection of both carbon and manganese and since the ternary interaction between manganese and carbon is attractive, we may expect the positive manganese 'spike' at the interface to retard the flow of carbon away from the interface and thus also retard the growth at certain stages of transformation [18].

Purdy et.al.[18] have shown using Kirkaldy's [19] general solution to the multi component diffusion equation, that when the interface is in complete equilibrium the transformation may occur with or without alloying element partition. At low supersaturation (where there is very low growth rate), manganese partitions to the austenite and ferrite growth is controlled by manganese diffusion in the austenite ahead of the interface. At higher supersaturation the transformation, while still maintaining complete equilibrium at the interface, is much faster, the rate being controlled by carbon diffusion and transformation being characterized by absence of measurable manganese partition.

According to the local equilibrium theory for growth into an infinite medium, there exist two regimes which are defined by the relative supersaturation. For high supersaturation, as indicated in Fig.2.3 [20] the rate equations with  $D_C \gg D_Mn$  imply that there is no partition of manganese between the austenite and the ferrite. On the other hand in the low supersaturation regime, partition must occur and diffusion control by the slowly-diffusing element takes over [21].

#### 2.8.2 Manganese Partitioning During the Austenite-Perlite Transformation :

All alloying elements in steels, with the exception of cobalt, retard the pearlite transformation. The austenite stabilizing elements like Mn, Ni etc. decrease the eutectoid temperature ( $A_{e1}$ ) and hence are generally expected to retard the pearlite transformation because of the decreased thermodynamic driving force for the transformation. The ferrite stabilizing elements like Mo, Cr, Si etc. increase the  $A_{e1}$  temperature. In their presence, pearlite transformation starts at temperature higher than the binary  $A_{e1}$  temperature. However, at lower temperatures the transformation rates are generally slower than the plain carbon eutectoid steel [22].

It is now generally agreed that during pearlite growth the alloying element partition between ferrite and cementite at low supersaturations and growth is controlled by alloying element boundary diffusion, whereas at high supersaturation pearlite growth occurs without any partitioning of alloying element and is controlled by carbon volume diffusion [23], [24], [25].

Razik et.al. [26] have studied the partitioning of Mn in Fe-C-Mn system and led to following conclusions.

During the austenite-pearlite transformation in eutectoid steels containing manganese, the manganese partitions preferentially to the pearlitic cementite

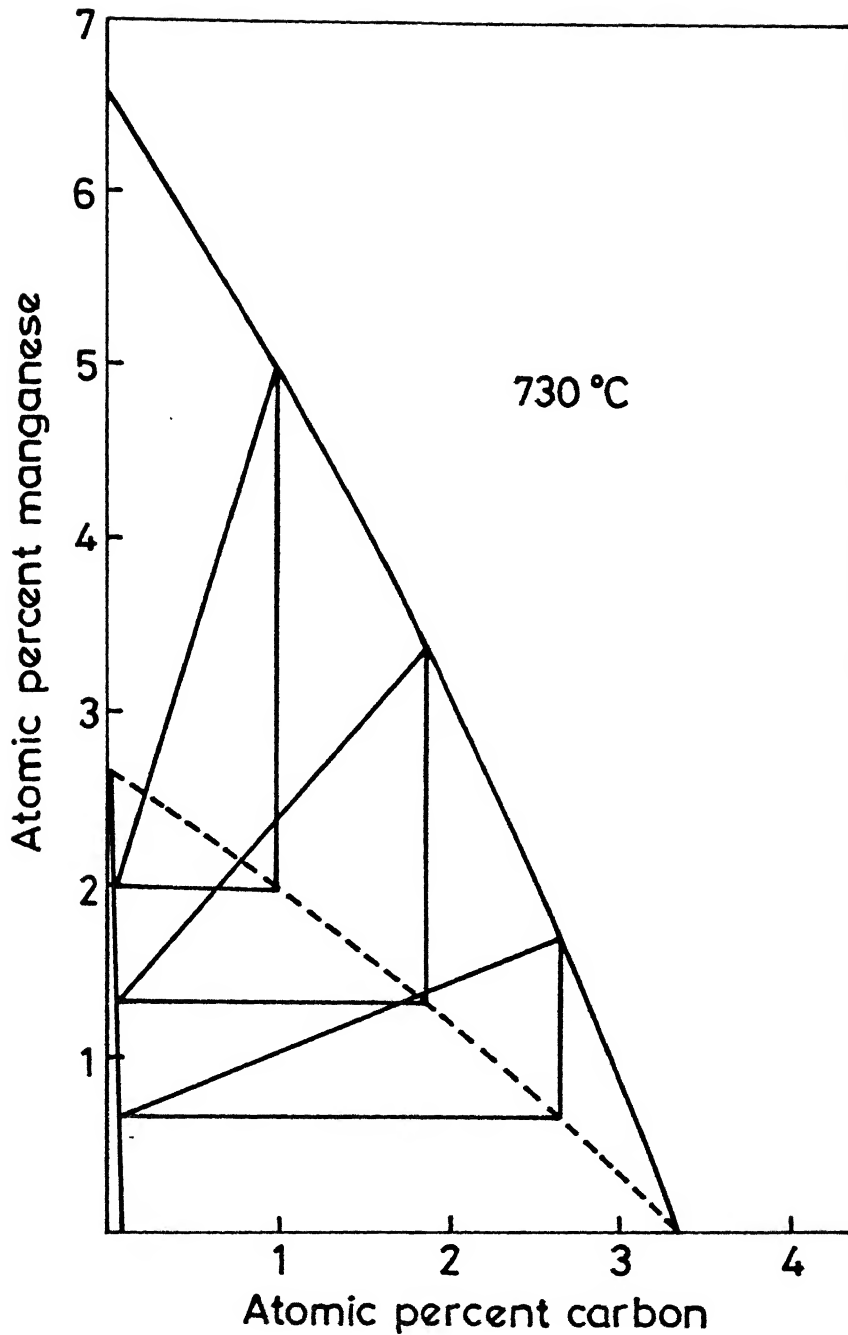


Fig. 2.3 730 °C isotherm for iron-rich alloys in the Fe-C-Mn alloy systems. The right triangles with tie-lines on the hypotenuse approximately define the boundary (----) between partition and no-partition reactions. [20]

at the transformation interface above a certain temperature (no-partition temperature) which depends on composition. The no-partition temperature  $T_p$  measured for steels containing 1.08 pct Mn and 1.80 pct Mn were 683 and 649<sup>0</sup>c respectively (Fig.2.4).

The partition coefficient at the austenite-pearlite interface increases with increasing transformation temperature and the indications are that equilibrium partitioning will occur at the interface at 712 and 693<sup>0</sup>c for the 1.08 and 1.80 pct Mn steels respectively (Fig.2.5). Manganese continues to segregate to cementite behind the austenite-pearlite interface while pearlite formation is still occurring and after it is complete until the concentration reaches its equilibrium value. The equilibrium partition coefficient decreases with increasing temperature.

The calculation of pearlite growth rates at temperatures below  $T_p$  using the assumption of either volume diffusion or interfacial diffusion of carbon as rate controlling led to calculated growth rates which only differ from those observed experimentally by a factor of 1-3 (see fig.2.6). Hence both volume and interfacial diffusion of carbon are equally probable and may occur simultaneously.

The marked influence of manganese additions on pearlite growth kinetics below  $T_p$  is due primarily to the effect of alloy element on the carbon concentration gradient, which is proportional to the driving force, at the transformation front. The reduced driving force has the effect of reducing the growth rate and increasing the interlamellar spacing for a given reaction temperature.

### 2.8.3 Kinetics of Austenite Formation in Steel with Ferrite-Pearlite

#### Microstructure :

The kinetics of austenite formation have been studied by Speich

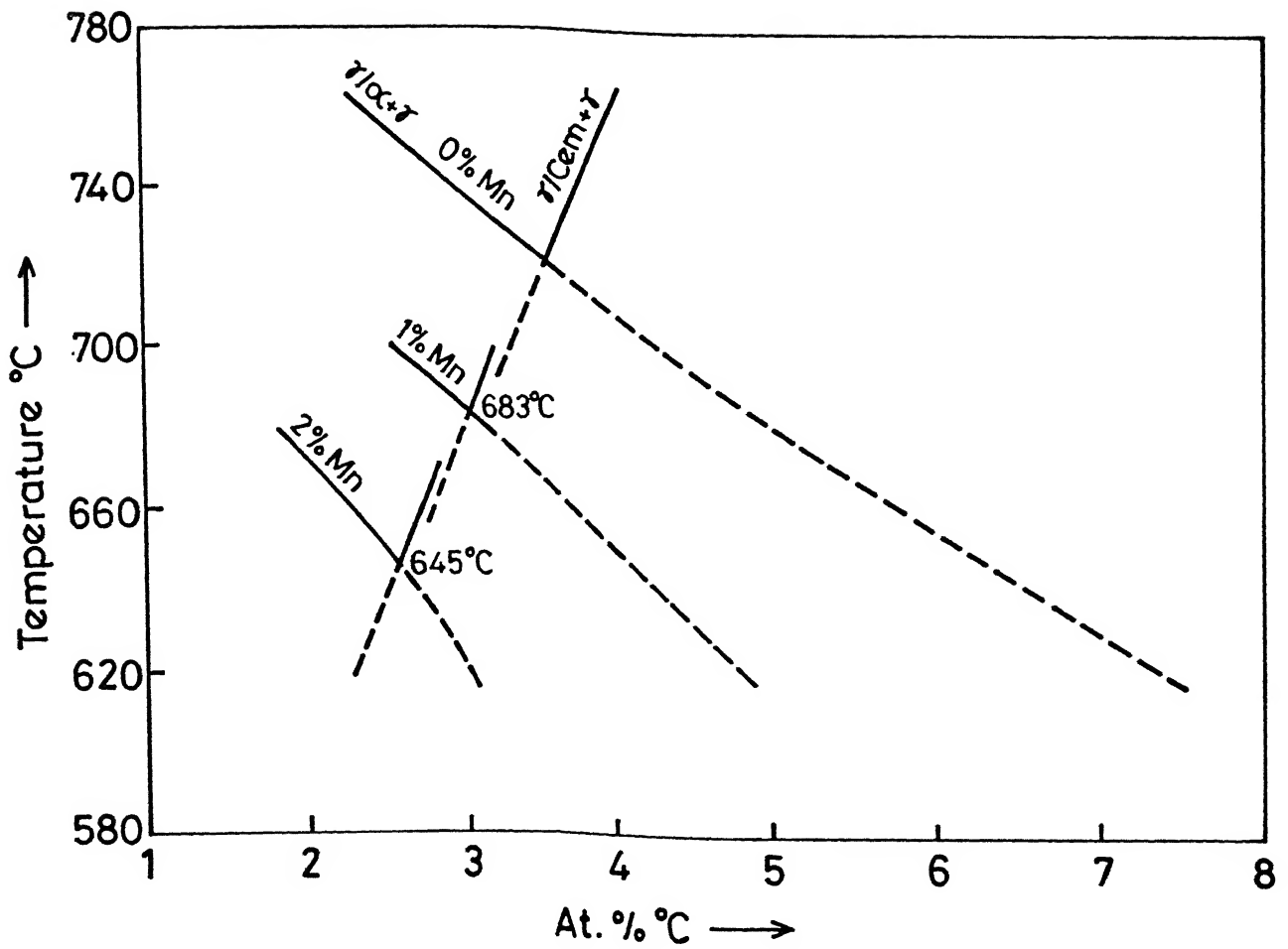


Fig. 2.4 Calculated no-partition phase boundaries for steels containing 0, 1 and 2% Mn [26].

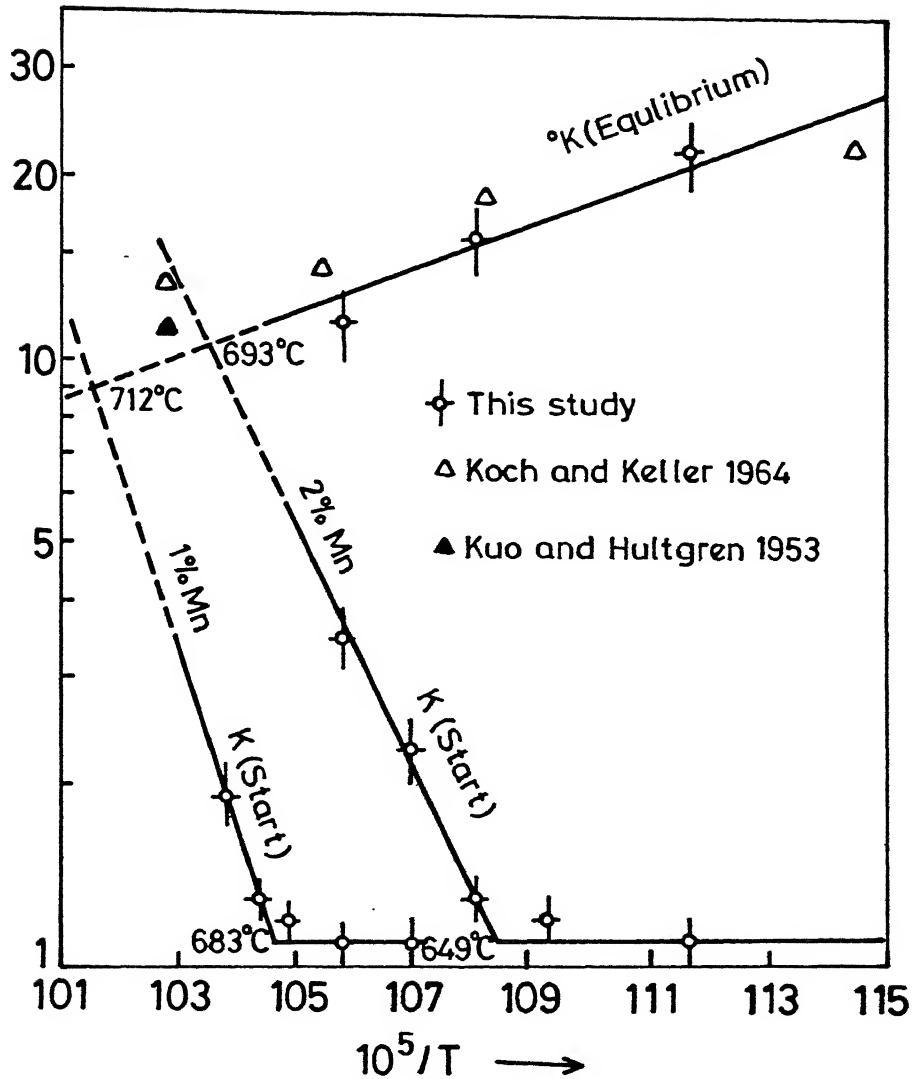


Fig.2.5 Logarithm of the partition coefficients of manganese vs reciprocal of the absolute temperature for the 1 Mn and 2% Mn steels. [26]

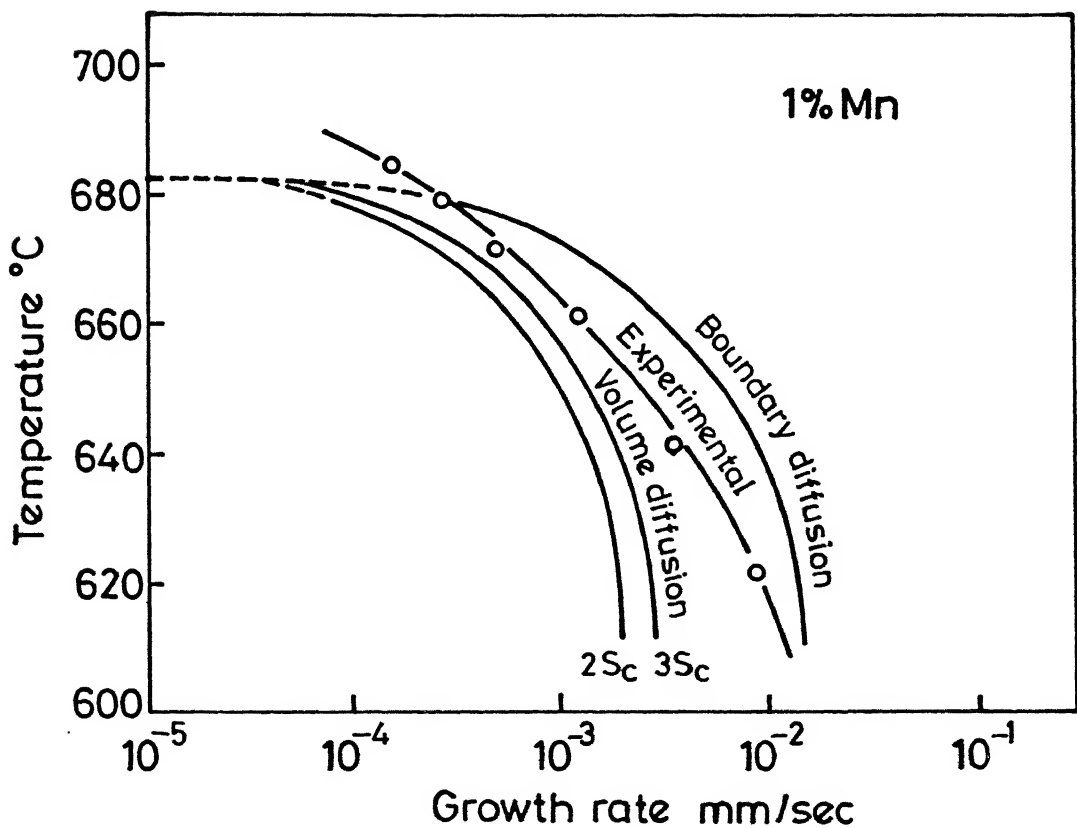


Fig.2.6 Calculated growth rates for the 1%Mn steel assuming volume diffusion or boundary diffusion of carbon as rate controlling mechanisms. [26]

et.al.[27] in three 1.5 pct manganese steels containing 0.06, 0.12 and 0.20 pct carbon and with a fine grained, unbanded ferrite-pearlite starting micro-structure. Kinetics of austenite formation has been shown in fig.2.7. A combination of dilatometric and quantitative metallographic techniques was used to establish the volume fraction of austenite in these steels after intercritical annealing at temperatures below  $740^{\circ}\text{C}$  and  $900^{\circ}\text{C}$ . The kinetics of austenite formation were separated into three steps.

1. Nucleation of austenite at the ferrite-pearlite interface and very rapid growth of austenite into pearlite, the times for complete dissolution of pearlite were very short (0.2 to 200 ms) at temperatures between 780 and  $900^{\circ}\text{C}$ . At temperatures between  $740^{\circ}\text{C}$  and  $A_{e1}$  the times for dissolution of pearlite became much (15 sec to 1 hour)
2. After dissolution of pearlite, further growth of austenite into ferrite occurred. At high temperatures of 850 to  $900^{\circ}\text{C}$ , the growth of austenite controlled by carbon diffusion in the austenite phase and the times for completion of this step were short (2 to 9 sec) at low temperatures between 780 and  $740^{\circ}\text{C}$ , the growth of austenite was controlled by manganese diffusion in the ferrite, and the times for completion of this step became much longer (4 to 24 hours).
3. Final equilibration of the manganese contents of the austenite and ferrite was controlled by manganese diffusion in the austenite, which is much slower process than manganese diffusion in ferrite. The times of completion of this process were extraordinarily long (2000 to 4000 hours).

Figure 2.8 is a schematic diagram of three steps in austenite growth



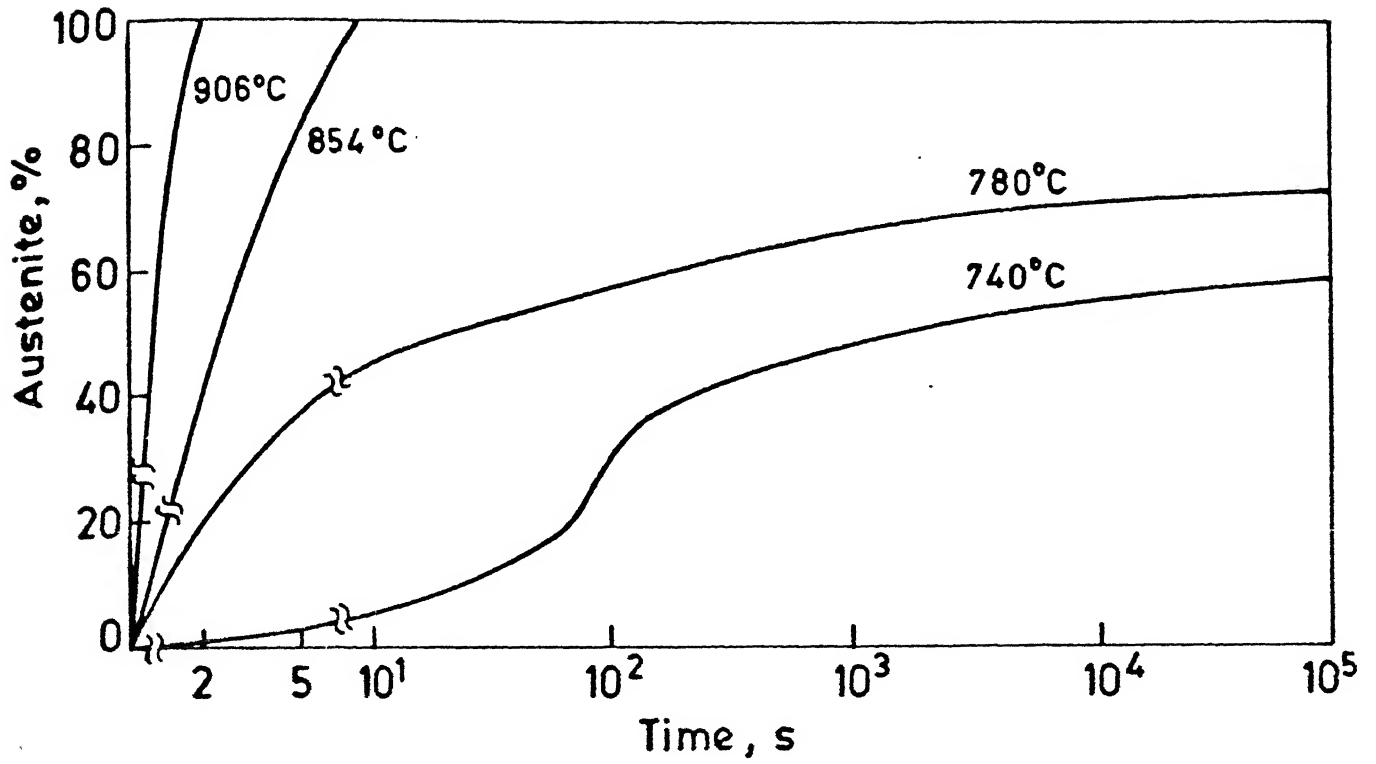


Fig. 2.7 Kinetics of austenite formation in 0.20 C-1.5 Mn steel [27]

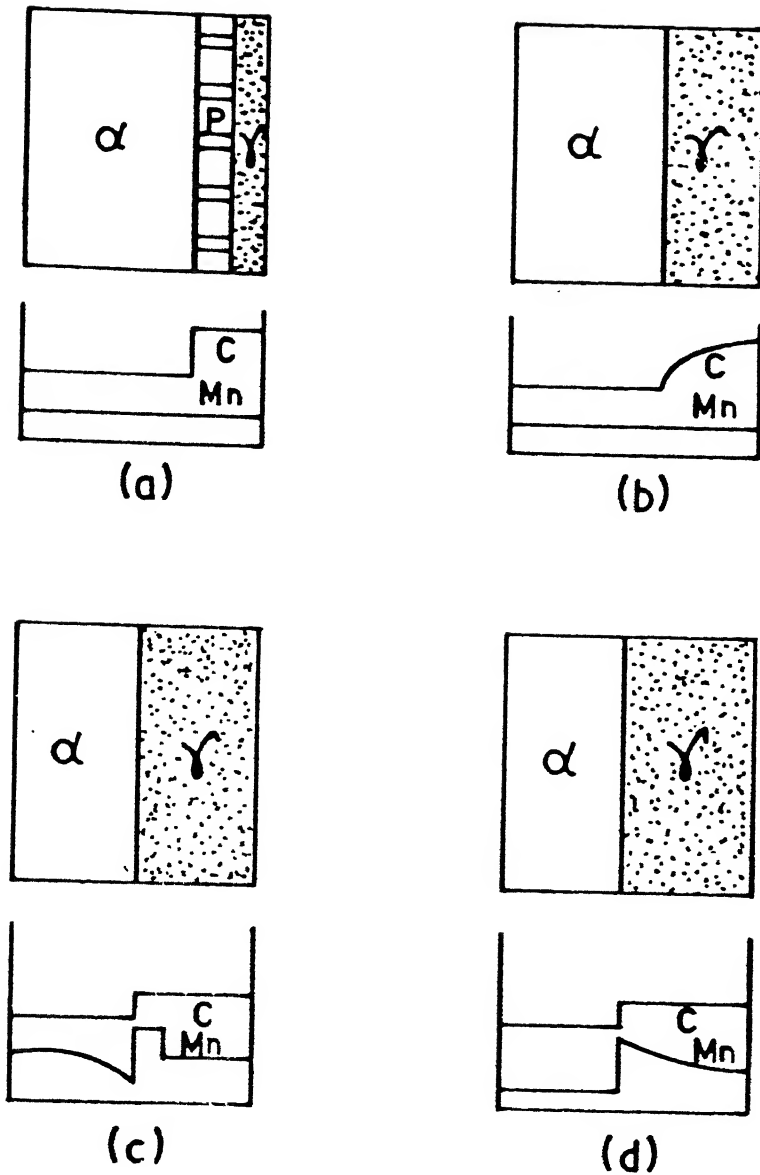


Fig. 2.8 Schematic diagrams of the three steps in austenite growth during intercritical annealing of ferrite-pearlite steels; (a) dissolution of pearlite; (b) austenite growth with carbon diffusion in austenite; (c) austenite growth with manganese diffusion in ferrite and (d) final equilibration with manganese diffusion in austenite. [27]

during intercritical annealing of ferrite-pearlite steels.

## 2.9 Thermal Cycling Treatment :

2.9.1 General - Thermal cycling treatment (TCT) with rapid heating, which is responsible for improvement of mechanical properties and lowering of critical embrittlement point [28], makes substantial changes to the structure of steel. Those include above all, a large decrease in the austenite grain size and, therefore, greater dispersity of the transformation product during quenching. At the same time, rapid heating can cause increased chemical inhomogeneity of the austenite [29].

### 2.9.2 Features of $\alpha$ - $\gamma$ Transformation in Engineering Steels Subjected to Thermal Cycling :

Yachenko et.al.[30] studied phase and structural transformation during thermal cycling treatment in the widely used engineering steels 15 Kh. and 40 Kh. with different critical points and different  $A_{e1}$ - $A_{e3}$  widths. The investigations were conducted on hot rolled products with a relatively homogeneous ferrite-pearlite structure.

It was found that single heating in all the thermal cycling schedules results in the formation of large masses of  $\gamma$ -phase composed of several grains. Subsequent repeated heatings results in phase transformation in the same locations, which involves only the adjacent areas of matrix in this process. The  $\gamma$ -phase masses become fragmented. This can be attributed to the fact that the formation of austenite in the intercritical temperature range occurs primarily in areas of high energy, while repeated heatings into the phase transformation range increase the number of these areas.

Thermal cycling treatment involving heating into the intercritical range also induces changes in the ratio of phases set by quenching. In

a ferrite-martensite structure for instance, the amount of martensite decreases with an increasing number of heating-cooling cycles. After single heating of 15 Kh. steel to 830-840<sup>0</sup>C, 94% martensite was 'fixed' by quenching and thermal cycling reduced this content to 73% with exposure of ferrite grains. One of the reasons for this reduction in martensite content is a reduction in austenite stability.

Thermal cycling of fine grained 15 Kh. and 40 Kh. steels with an initial grain size of  $16 \times 10^{-3}$  mm and  $13 \times 10^{-3}$  mm therefore causes no marked refinement of the grain structure. The maximum grain refinement was obtained as a result of thermal cycling treatment with the following schedule,  $A_{e_3} - (10-20^0\text{C}) \rightleftharpoons 20^0\text{C}$ . The grain size after five fold heating of 15 Kh. & 40 Kh. steels were  $8 \times 10^{-3}$  mm and  $10 \times 10^{-3}$  mm respectively.

### 2.9.3 Transformation Kinetics of the Austenite of Engineering Steels During Thermal Cycling Treatment :

The influence of thermal cycling treatment on the kinetics of the isothermal transformation of austenite was investigated by Konopleva et.al. [31] in low carbon high duty steel 08 Kh.2G 2F composition in wt.pct. C-0.093, Si-0.57, Mn-2.0, Cr-2.06, V-0.135, Al-0.028, S-0.006, hot rolled. The TCT programme consisting of three cycles of rapid heating and quenching from temperature in cycle I-950, II-900, \* For comparison, they studied the transformation kinetics of the austenite after normal heating in furnace for 15 minutes at 950<sup>0</sup>C.

They found that the maximum of the size distribution curve of the austenite grain after TCT is at 3  $\mu\text{m}$  and after normal heat treatment at 12  $\mu\text{m}$  as shown in fig.2.9. The scatter of sizes in the fine grained specimens is much less indicating a greater degree of uniformity in resulting

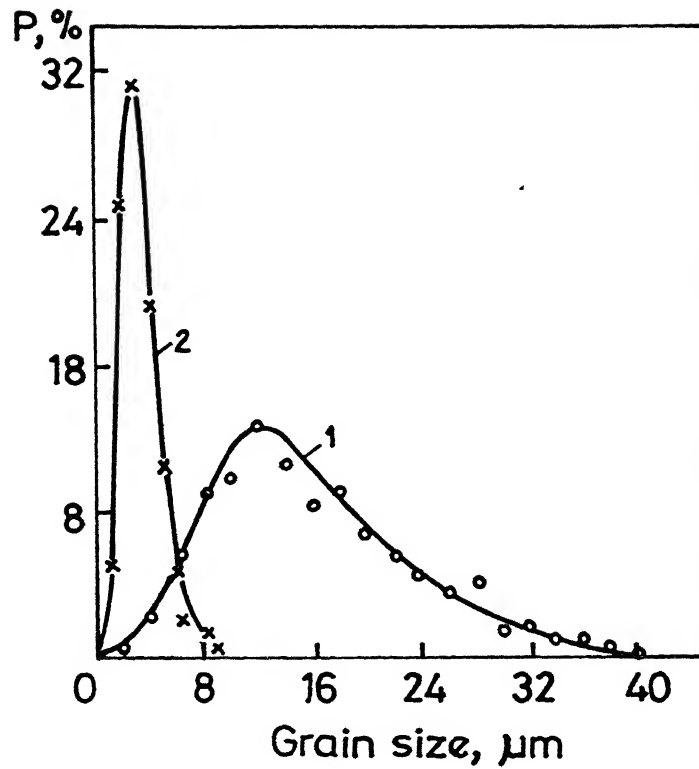


Fig.2.9 Frequency distribution of size of austenite grains of steel 08Kh2G2F. 1-heating 950°C, 15min; 2-TCT. [31]

structure. After normal heating ( $950^{\circ}\text{C}$ ) the austenite has enhanced stability at the temperature of ferrite pearlite transition (see fig.2.10).

Refinement of the structure of the steel as a result of TCT greatly accelerated the ferrite-pearlite transformation (see figs.2.10 2.11). The structure of specimens after isothermal holding at  $600-680^{\circ}\text{C}$  consisted of excess ferrite and pearlite. After thermal cycling treatment, all the structure components had a higher degree of dispersity. The kinetic curves of austenite decomposition at  $600-680^{\circ}\text{C}$  have well expressed points of inflexion (arrowed in fig.2.11). The method of trial quench was used to establish that the ferrite forms in the specimen before the point of inflexion and pearlite after it. A comparison of the kinetic curves of austenite decomposition shows that accelerating effect of thermal cycling treatment on the ferrite transformation increases by a factor of two (relative to 5% transformation) when the isothermal holding temperature is raised from  $600-680^{\circ}\text{C}$ .

The factors which condition the change of the austenite transformation kinetics during thermal cycling treatment (grain refinement, chemical inhomogeneity, increased structural imperfections), usually assisting the transformation of austenite in the ferrite-pearlite range. So highest rate of the transformation at  $600-680^{\circ}\text{C}$  was observed in specimen with finely dispersed structure obtained as a result of TCT and the slowest after high temperature holding at  $1100^{\circ}\text{C}$  as evident from fig. 2.11, producing uniform large-grained austenite.

The substantial growth of austenite grain with rise of heating temperature from  $950-1100^{\circ}\text{C}$  delays the ferrite transformation relatively little. Probably the effectiveness of influence of grain size on the kinetics is complicated by the process of precipitation of the carbonitride phases from supersaturated solid solution, the formation of which is possible at temperatures of the diffusion transformation of austenite ( $600-680^{\circ}\text{C}$ )

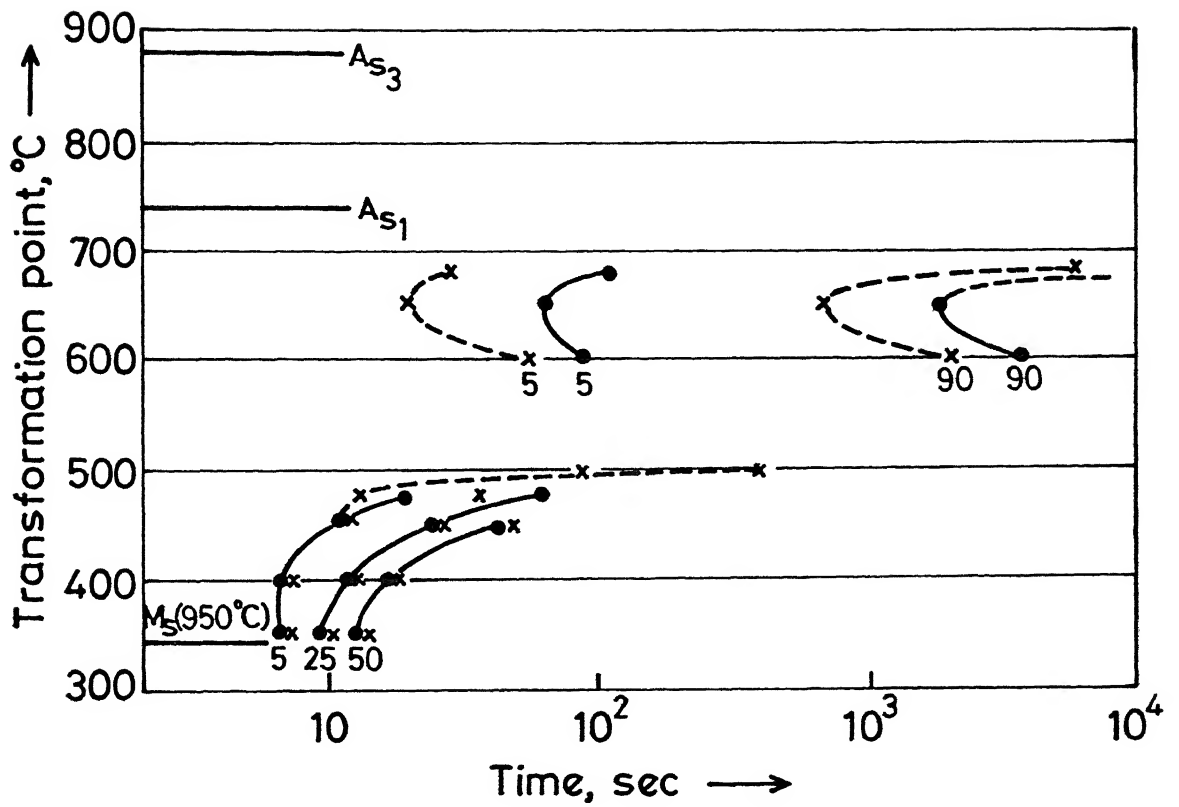


Fig.2.10 Isothermal transformation of austenite of steel 08Kh2G2F: ----HCT. — heating  $950^\circ\text{C}$ , 15 min. Numbers on curves extent of transformation, %. [31]

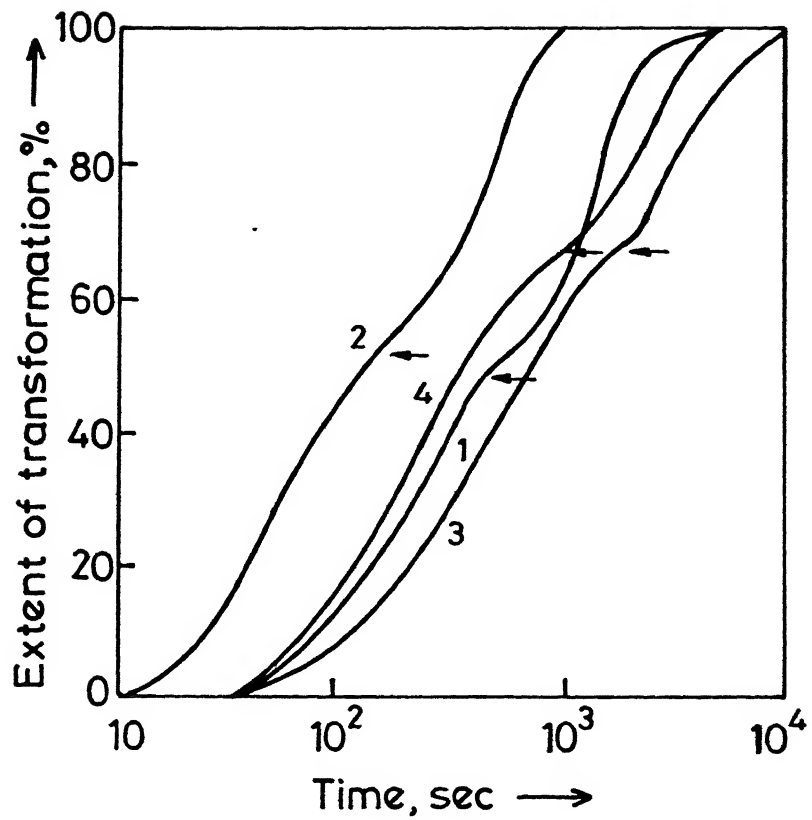


Fig. 2.11 Kinetics of ferrite-pearlite transformation of austenite of steel 08Kh2G2F at 650° :  
1-heating 950°, 2-HCT, 3-heating 1100°,  
4-heating 1100°, staged holding 950°C [31].



#### 2.9.4 Diffusion During the Thermal Cycling\* Steels : of

An investigation by Zobel et.al.[32] was conducted to assess the effect of thermal cycling on carbon diffusion in steel. Isotope-tracer experiments were carried out on specimens (20mm dia, 20mm long) of steel containing 0.21 pct C, 0.23 pct Si, 0.42 pct Mn; Vacuum annealed at 1273 K for 4 hours. It is found that thermal cycling with partial or complete phase transformation produces a factor of 2.5-3 increase in the diffusion mobility of carbon atoms. The observed acceleration in the diffusion process is ascribed to the combined effect of the following factors; grain refinement, phase recrystallization, internal stress generation and relaxation, lattice defects and thermal diffusion.

#### 2.9.5 Effect of Thermal Cycling on Mechanical Properties of Steels :

A thermal cycling treatment (heating at 5°C per minute to a temperature of 5-10°C above  $A_{c3}$  with subsequent aircooling to a temp. of 5-10°C below  $A_{r1}$  for three to five cycles) of 20 Kh steel resulted in grain refinement to No.1 and impact resistance after final cooling was 1.5-2.5 times higher than that obtained after normalization and thermal cycling treatment at high rates of heating. The slow heating and cooling rates in the new treatment prevented phase transformation hardening [33].

In another study [34] accelerated thermal cyclic heat treatment of 40 Kh steel was carried out in order to assess its effect on fatigue limit, fatigue limit obtained was 100% higher than that obtained after conventional furnace reheating.

Sopockin et.al.[35] studied the effect of various modes of thermocyclic treatment on mechanical properties of reactor vessel steel. The steel samples (160 mm thick) were (i) normalized (ii) thermocycled in salt bath with

a subsequent water cooling and (iii) thermocycled in a gas box furnace with air cooling, and then were subjected to metallographic examination, mechanical tests for tensile strength characteristics and impact strength. A typical recrystallization during either of the themocyclic treatment resulted in the formation of fine grained structure which led to an increased impact strength of the steel and shifted its transition temperature down by 25<sup>0</sup>c as compared to normalization.

CENTRAL LIBRARY  
Acc. No. **105933**

## CHAPTER-3

### EXPERIMENTAL PROCEDURE

#### 3.1 Selection of Material :

Our purpose in this investigation was to study the effect of thermal cycling through phase transformation on diffusion in steels and subsequently on microstructural banding. For this purpose we prepared diffusion couples of alloy layers of compositions shown in table 3.1. The composition of the steel with banded ferrite-pearlite microstructure was C=0.3 pct and Mn=0.8 pct.

Figure 3.1 and 3.2 are the representative photomicrographs of alloy plates used for making the diffusion couples. Fig. 3.3 is the representative photomicrograph of rolled banded steel specimen.

Table 3.1

Steel	C	Si	S	P	Mn.
N <sub>2</sub>	0.05	0.2	0.02	0.02	0.08
N <sub>15</sub>	0.31	0.29	0.038	0.03	0.84

#### 3.2 Preparation of Diffusion Couples :

To prepare the couples the steels of composition N<sub>2</sub> & N<sub>15</sub> were cold rolled to various thickness, varying from 0.20 to 0.65 mm. After cleaning, the layers were clamped in an assembly (shown in fig.3.4) in sets of three plates (keeping the plate of composition N<sub>15</sub> in between the two plates of composition N<sub>2</sub>) to form the couples. The layers were separated from the assembly plates with the help of mica sheets. The whole assembly was vacuum sealed in quartz capsules. Welding was effected by annealing at temperatures 900, 950 & 1000°C for varying periods, each time couples were taken out of assembly, polished and observed under optical microscope.

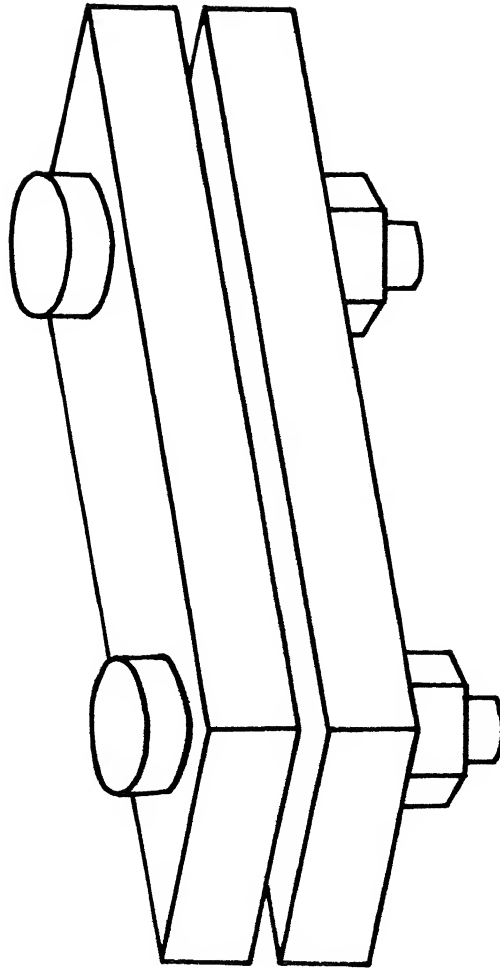


Fig.3.4 Assembly used to prepare diffusion couples.

Welding was found good after annealing for sevendays at  $950^{\circ}\text{C}$  and excellent after annealing for sevendays at  $1000^{\circ}\text{C}$ . The two couples used for further studies were prepared by annealing for sevendays at  $950$  and  $1000^{\circ}\text{C}$  respectively and indentified as diffusion couple I and diffusion couple II for further reference.

The figure<sup>3.5</sup>\* is a photomicrograph of a typical diffusion couple. It consisted initially of an alloy layer of composition  $N_{15}$  sandwiched between two layers of plain carbon steel of composition  $N_2$ .

### 3.3 Heat Treatment of Diffusion Couples :

The couples were cut into four pieces with the help of a diamond cutter. The parts were identified as 1,2,3&4 for future reference. The piece 1 of all the couples were retained as it is. The piece 2,3&4 were subjected to various heat-treatments after vacuum sealing .

#### 3.3.1 Annealing Treatment :

Annealing was carried out at  $950^{\circ}\text{C}$  as per the following schedule

Table 3.2

Diffusion Couple	Piece No.	Total duration (days)
I	2	6
II	2	12

Samples were polished successively on 0,00,000 & 0000 emery papers, wheel polishing was carried out using alumina powder of  $0.3\text{ }\mu\text{m}$ . Etching was done using 5% nital. The specimens were observed under optical microscope.

#### 3.3.2 Thermal Cycling Treatment :

Thermal cycling treatment was first tried with the help of ordinary tube furnace, but it was found very difficult to keep constant cooling and



Fig.3.5 The micrograph of typical diffusion layer couple showing simulated banding effect near welds.(X 100, Enlarged 4 times)

and heating rates. So finally thermal cycling was carried out with the help of differential thermal analyser (D.T.A.) equipment, which consists a furnace with computerised controles. D.T.A. equipment was programmed for thermal cycling treatment. The extreme temperatures were set at 600 and 950<sup>0</sup>c with the holding time of 10 minutes at the extremes and heating and cooling rates were set at 10<sup>0</sup>c/Min.

Thermal cycling treatment was carried out between temperatures 600<sup>0</sup>c and 950<sup>0</sup>c at constant heating and cooling rates of 10<sup>0</sup>c/Min and holding for the ten minutes at the extreme temperatures. A typical cycle has been shown in fig.3.6. The couples were given thermal cycling treatment as per the following schedule.

Table 3.3

S.No.	Diffusion Couple	Piece No.	No.of Cycles	Total duration (Days)
1	I	3	50	3
2	I	4	100	6
3	II	3	100	6
4	II	4	200	12

The samples were polished successively on 0,00,000, and 0000 emery papers. Wheel polishing was carried out using alumina powder of 0.3 um. Etching was done using 5% nital solution. The specimens were observed under optical microscope. Diffusion couple I piece 3 got oxidised, most probably due to improper vacuum sealing and had to be discarded at this stage only.

#### 3.4 Treatment of Steel With Banded Microstructure :

A specimen of steel containing ferrite pearlite banding (shown in fig.3.3) of size 15x15x15 mm was taken. It was cut into four parts identified as 1,2,3, & 4, for future reference. Part '1' was not subjected to any

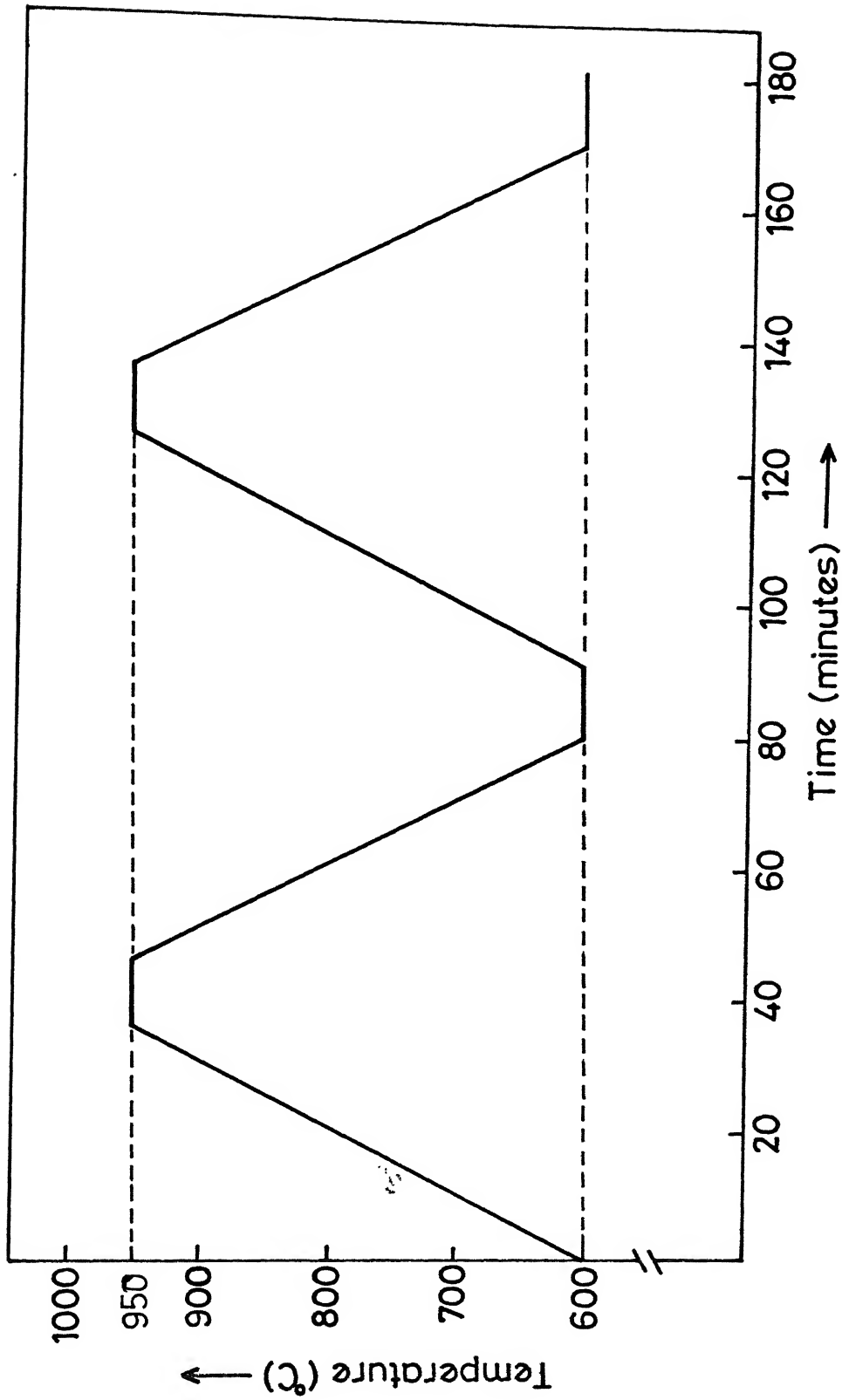


Fig.3.6 Thermal cycling schedule for the experiment.



further heat treatment. Part '2' was annealed for 6 days at 950°C. Part '3' was thermal cycled with the help of D.T.A. equipment between 600 and 950°C at constant heating and cooling rates of 10°C/Min, and holding for ten minutes at the extreme temperatures, the total number of cycles were 50 and total duration was 3 days. Part '4' was thermal cycled with the same cycle as for part '3' but for 100 cycles and total duration was 6 days.

All the above specimens were polished successively on 0,00,000 & 0000 emery papers. Wheel polishing was carried out using alumina powder of 0.3 µm. Etching was done using 5% nital soln. The specimens were observed under optical microscope.

### 3.5 Electron Probe Micro Analysis :

All the specimens were again polished and Mn. profiles across the cross-section were calculated with the help of Electron Probe Micro Analysis (EPMA) at RDCIS Ranchi.

The various results have been shown and discussed in the next chapter.



Fig.4.1 The micrograph of simulated diffusion layer couple I  
(X 100, Enlarged 4 times)

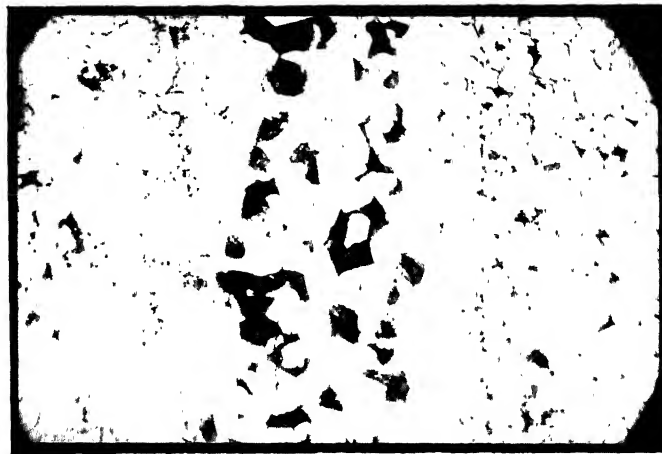


Fig.4.2 The micrograph of diffusion couple I  
annealed for 6 days at 950°C  
(X 100, Enlarged 4 times)

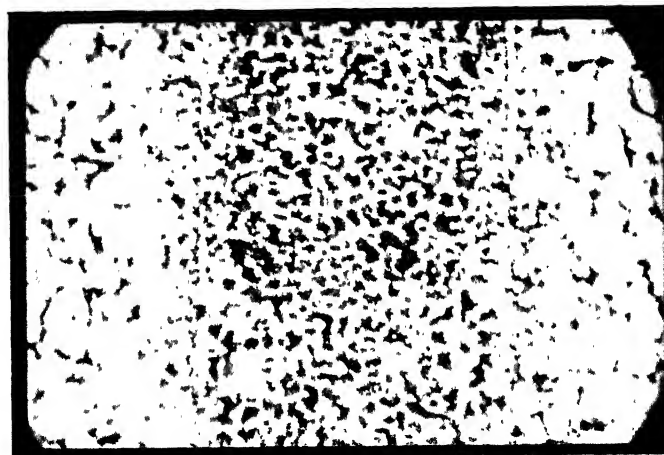


Fig.4.3 The micrograph of diffusion couple I  
thermal cycled for 100 cycles



Fig.4.4 The micrograph of simulated diffusion layer couple II.  
(X 100, Enlarged 4 times)

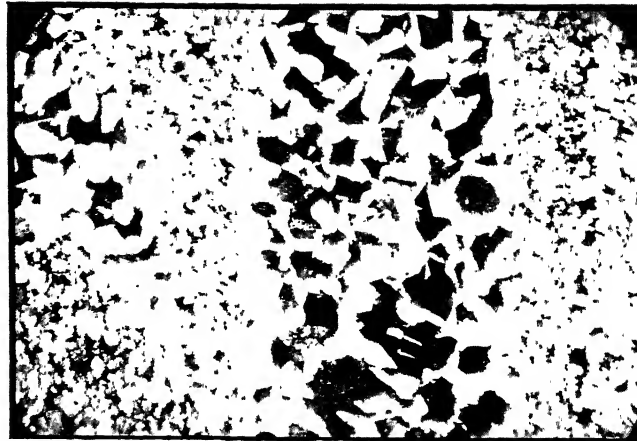


Fig.4.5 The micrograph of diffusion couple II annealed for 12 days at 950°C.  
(X 100, Enlarged 4 times)

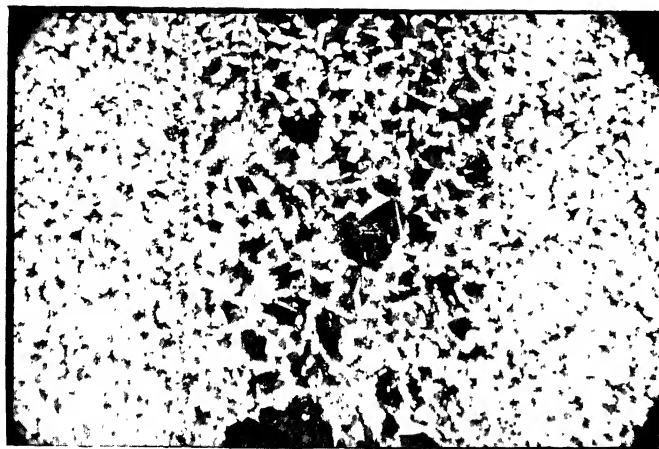


Fig.4.6 The micrograph of diffusion couple II thermal cycled for 100 cycles.  
(X 100, Enlarged 4 times)

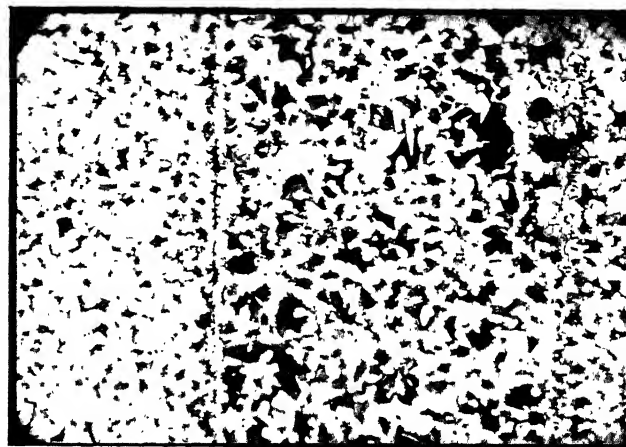


Fig.4.7 The micrograph of diffusion couple II thermal cycled for 200 cycles.  
(X 100, Enlarged 4 times)

for 100 cycles (total duration 6 days). It shows distinct reduction in grain size throughout. Though the concentration of pearlite is much higher in central region, yet there is no pearlite free band in the structure.

7. Fig.4.7 is the photomicrograph of diffusion couple II thermal cycled for 200 cycles (total duration 12 days). It shows fine grained, ferrite-pearlite microstructure, almost uniform throughout the structure.
8. Fig.4.8 is the photomicrograph of a rolled low C-Mn steel. It shows ferrite-pearlite microstructural banding in commercial steels.
9. Fig.4.9 is the photomicrograph of same steel (shown in fig.4.8), annealed for 6 days at 950°C. It shows large, ferrite & pearlite grains.
10. Fig.4.10 is the photomicrograph of same steel (shown in fig.4.8) thermal cycled for 50 cycles (total duration 3 days). It shows distinct reduction in grain size. It is also observed that interband spacing has reduced considerably.
11. Fig.4.11 is the photomicrograph of same steel (shown in fig.4.8) thermal cycled for 100 cycles (total duration 6 days) It shows further reduction in grain<sup>size</sup> and interband spacing.

#### 4.2 Electron Probe Microanalysis :

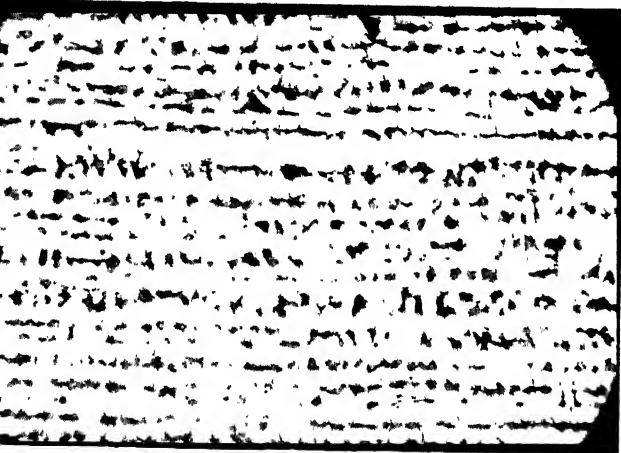
1. Fig.4.12 is Mn-profile for simulated diffusion couple II. It shows that the general profile has elevated in the middle region in addition to the presence of some peaks.
2. Fig.4.13 is Mn-profile for simulated diffusion couple II annealed for 12 days at 950°C. It again shows elevated profile in the middle portion in addition to some peaks but the length of elevated portion has reduced as compared to fig. 4.12.



4.8 The micrograph of rolled low C- Mn steel  
(X 100, Enlarged 4 times)



Fig.4.9 The micrograph of rolled low C- steel annealed for 6 days at 950  
(X 100, Enlarged 4 times)



.10 The micrograph of rolled low C- Mn steel thermal cycled for 50 cycles  
(X 100, Enlarged 4 times)

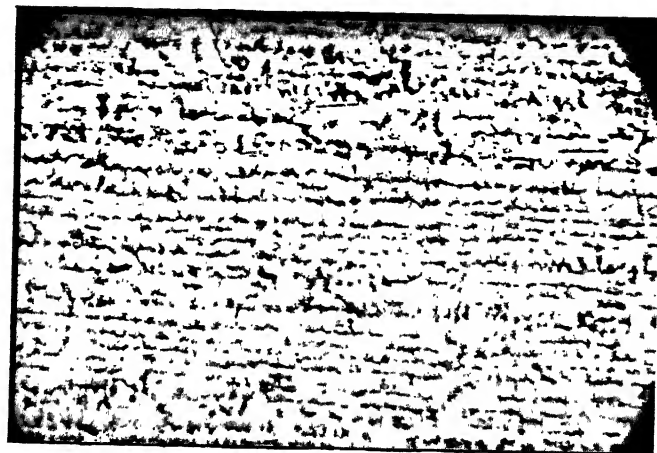


Fig.4.11 The micrograph of rolled low C-Mn steel thermal cycled for 100 cycles  
(X 100, Enlarged 4 times)



Fig.4.12 The Mn-profile for simulated diffusion layer couple II  
(X 400, Enlarged 2 times)



Fig.4.13 The Mn-profile for diffusion couple II annealed for 12 days at 950°C  
(X 400, Enlarged 2 times)



Fig.4.14 The Mn-profile for diffusion couple II thermal cycled for 100 cycles  
(X 400, Enlarged 2 times)



Fig.4.15 The Mn-profile for diffusion couple II thermal cycled for 200 cycles  
(X 400, Enlarged 2 times)

3. Fig.4.14 is Mn-profile for diffusion couple II thermal cycled for 100 cycles, total duration 6 days. It shows a very few peaks of Mn and also they<sup>are</sup> very small.
4. Fig.4.15 is Mn-profile for diffusion<sup>couple</sup> II thermal cycled for 200 cycles, total duration 12 days. It shows only one, very small Peak of Mn.

#### 4.3 Discussion :

Our initial efforts had been to make a good simulation of ferrite-pearlite microstructural banding in steels. Photomicrographs 4.1 and 4.4 shows the pearlite distribution over most of area of layers while banding in both weld zones, where the alloy gradients are steep. A typical diffusion couple has been formed. This shows a good simulation of microstructural banding.

Diffusion annealing, to form the couples, was carried out for 7 days at 1000°C, the diffusion length of carbon  $2\sqrt{Dt}$  was 8.23 mm (here D was calculated by putting  $D_0=0.2 \times 10^{-4}$  M<sup>2</sup>/sec and  $Q=142$  KJ/mole for C in Fe( $\gamma$ ) and  $T=1273^{\circ}\text{K}$  in  $D=D_0 e^{-Q/RT}$ ). Which is around 21 times the thickness of an individual layer. This is more than sufficient time for carbon to attain a transient equilibrium distribution with respect to the substantially static distribution of the substitutional component [36]. Accordingly we can not attribute the intense segregation which occurs in the room temperature microstructure of banded steels to the segregation of carbon. However, Mn which is still segregated (as its diffusion length  $2\sqrt{Dt}$  was only 0.31 mm which was calculated by using 'D' austenetic diffusion coefficient of Mn at  $1273^{\circ}\text{K}=4.1 \times 10^{-10}$  Cm<sup>2</sup>/sec). significantly influences the difference in  $A_{e3}$  temperature between adjacent layers and with it the sequence of

ferrite nucleation across diffusion couple. As Manganese decreases  $A_{e_3}$  line and activity of carbon in austenite, figure 4.16 [3] has been constructed to describe the sequence of events which occurs during cooling. Fig. 4.16(a) indicates the activity build up about nuclei of ferrite which have appeared in Mn-free region on cooling to  $A_{e_3}$  temperature of Fe-C system. On further cooling to the  $A_{e_3}$  temperature of Fe-C-Mn system, similar nuclei appear in Mn-rich region as indicated in fig. 4.16 (b). In the meantime the original ferrite nuclei have grown, building up the austenite carbon concentration and therefore the activity. In regions far from the weld carbon diffusion fields about ferrite regions interfere with each other and restrict the growth to within the bands provided by the lever-rule. On the other hand, precipitate near the weld can pump excess carbon into the ever-deepening sink on the untransformed side of the weld, thus growing indefinitely without reference to lever rule. Fig.4.16 (c) indicates the configuration attained at the eutectoid temperature for the Mn-free layers. This layer has now attained substantially uniform activity with approximate lever rule quantities of austenite and ferrite every where but near the weld. At that line there is a pure ferrite band and adjacent to it a carbon rich austenite layer which on final transformation is enriched in pearlite as indicated in the schematic micrograph of fig. 4.16 (d).

The effects of annealing treatment are shown in photomicrographs 4.2,4.5,4.9 and fig. 4.13, there is some increase in the carbon content of ferrite region and decrease in length of elevated portion (Mn-rich region) of Mn-profile. Due to the concentration gradient between pearlite and ferrite bands and high temperature, diffusion of Mn has occurred. However, even after 12 days at 950°C. homogenization has not been effected to such an



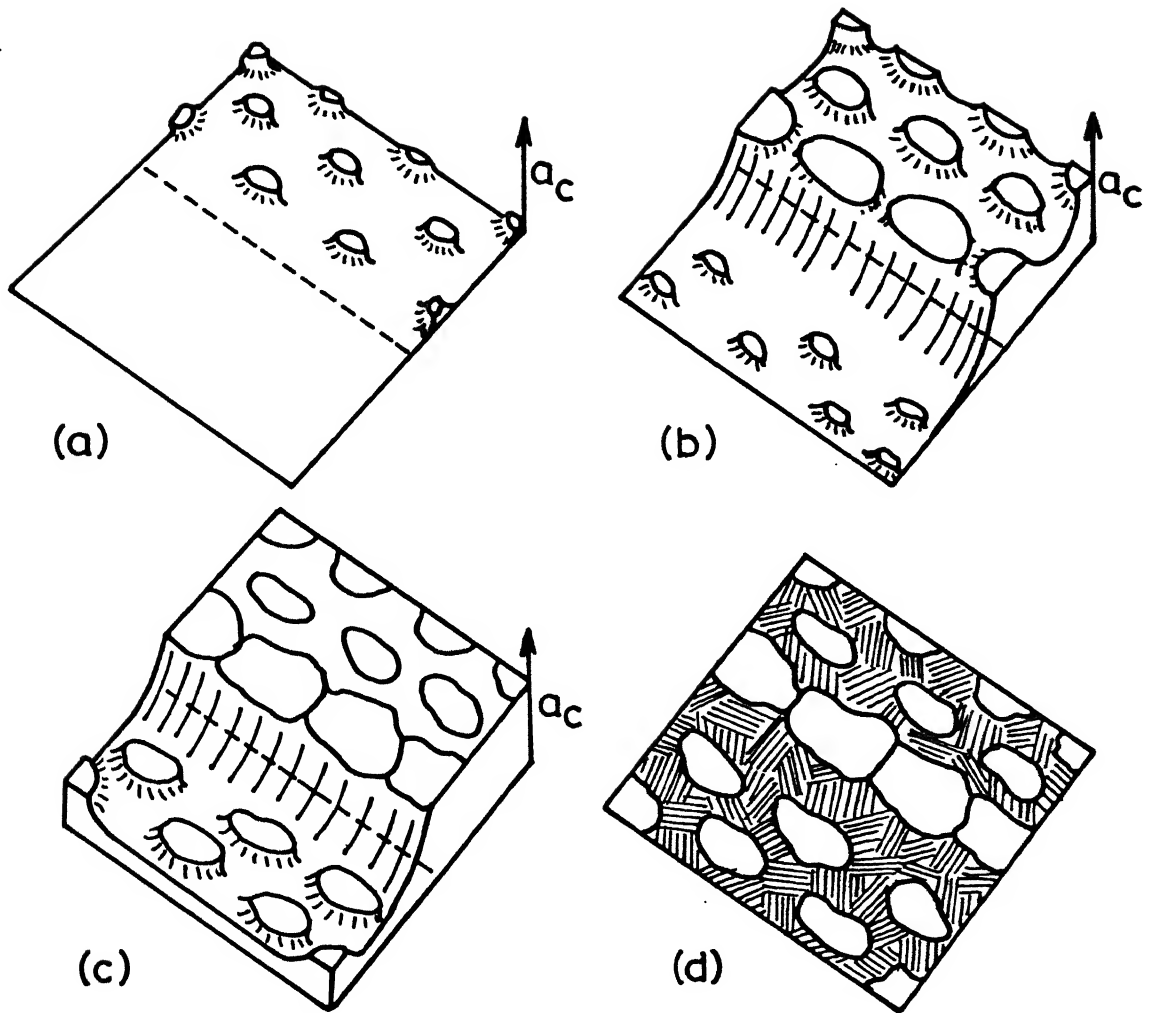


Fig.4.16 Schematic representation of the evolution of the activity surface of an Fe-C-Mn diffusion layer couple. [3]

extent so as to give an uniform distribution of carbon. In fact even after 12 days at 950°C, the banding is still evident, albeit with less clearly demarcated boundaries and increased carbon concentration in the ferrite bands (photomicrograph 4.5). This is due to very little diffusion of Mn, as diffusion length after 12 days calculated in <sup>the</sup> same way as in <sup>the</sup> previous case only 0.41mm, which is insufficient to equalize Mn activity throughout the couple. The effects of thermal cycling treatment are shown in photomicrographs 4.3, 4.6, 4.7, 4.10, 4.11 and figs. 4.14 and 4.15. Thermal cycling not only effects a better distribution of carbon and manganese, but also refines the grain size. It has been noted [37] that crystalline imperfections accumulate during thermal cycling treatment. An increase in the density of imperfection in the austenite significantly accelerates the precipitation of free ferrite in hypoeutectoid steels [38]. The decreased stability of austenite results in an increase in ferrite concentration at the centre. It has been clearly established that after single heating into the intercritical range, recrystallisation develops both in  $\alpha$  and  $\gamma$  phases [39]. Repeated alternating heating and cooling cycles led on the one hand, to increased holding at high temperature and, on the other, to phase work hardening. These two factors promote the development of recrystallisation process [30]. And recrystallization results in change in grain size. Maximum refinement of grains was obtained some where before 100 cycles with increase in the number of cycles there is hardly any change in grain size, only homogenization has been better effected in 200 cycles due to the increased time at high temperature.

The combined effect of the grain refinement, phase recrystallization, internal stress generation and relaxation, lattice defects and thermal diffusion during thermal cycling treatment increases the diffusion mobility during

thermal cycling, and that is why, much better homogenization is observed during thermal cycling as compared to annealing for the same duration. However this inference is purely based on qualitative analysis. The relative effect of thermal cycling treatment on diffusivity of substitutional alloying element with respect to annealing treatment could have been better established if we would have been able to perform the extensive quantitative analysis of Mn distribution after various treatments with the help of Electron Probe Micro Analyser and subsequently calculations of diffusivity, as we aimed while undertaking present investigation. However, due to the limited availability of Electron Probe Micro Analyser we had to restrict our investigations to qualitative analysis only.

CHAPTER - 5

**CONCLUSIONS**

- 1) Microstructural banding gets substantially reduced after thermalcycling treatment for 200 cycles between temperatures 600 and 950°C at the constant heating and cooling rates of 10°C/min. Whereas annealing treatment at 950°C for the same duration ( 12 days) has little effect on microstructural banding.
- 2) Thermal cycling treatment involving phase transformations results in marked refinement of grainsize. Maximum grain refinement was obtained some where before 100 cycles, the grain size tending to remain constant after additional cycling.
- 3) The qualitative analysis (Microstructural and Mn-profile analysis) indicates that thermal cycling treatment involving phase transformations results in higher diffusion mobility of substitutional alloying element Mn as compared to annealing treatment.

## REFERENCES

1. R.A. Grange; Metall. Trans., 1971. vol.2, p.417.
2. Yu. P.Gul, I.Z.Shukis, O.S. Williams, A.D. Kovaleva and A.A. Silchenko; Steel in the USSR, 1987, vol.17, p.140.
3. J.S. Kirkaldy, J.Von D. Foistmann and R.J. Brigham; Can.Met.Quart., 1962, vol.1, p.59.
4. C.F. Jatczak, D.J. Girardi and E.S. Rowland; Trans. A.S.M., 1956, vol.48, p.279.
5. A.Hays and J.Chipman; J.Trans. AIME, 1939, vol.135, p.85.
6. Basic Open Hearth Steel Making; AIME 1951, p.444.
7. M.Hansen; Constitution of Binary Alloys, Mc Graw-Hill, 1958.
8. C.J. Smithells; Metal Reference Book, 1955, vol.2, Butter Worths Sci. Publications.
9. W.A. Spitzig; Metall. Trans.A, 1983, vol.14A, p.271.
10. V.A. Kislik and A.I. Karmazin; Proizvod Zhelezn Droof Ral sov Koles, 1979, vol.7, p.88.
11. M.J. Laniessse, A.Peneau, and H.Aubert; Mem. Sci. Rev. Metall., 1979, vol.76, p.741.
12. P.K. Chatterjee, Parkt. Metallgr., 1979, vol.16, p.457.
13. D.Bhattacharya, M.Yanase, and S.Katayama; Strategies for Automation of Machining Materials and Processes, Orland, Florida, U.S.A., 5-7 May 1987, A.S.M. International, Metal Park, Ohio, U.S.A.
14. E.S. Dovenport; Trans. ASM, 1939, vol.27, p.837.
15. R.P. Smith; J.Am. Chem. Soc., 1948, vol.70, p.2724.
16. Yu.P. Gul; Auth. Cert, 730828 (USSR), Otkrytiya, Izobr., 1980, vol.16, p.114.
17. J.R. Bradely, G.J. Shiflet, H.I. Aaronson, Solid-Solid Phase Transformations,

Pittsburgh. Pa, 10-14 Aug. 1981, The Metallurgical Society/AIME.  
420 Common Welth, Dr. Warrendale Pa 15086, 1982.

18. G.R. Purdy, D.H. Weichert and J.S. Kirkaldy; Trans. TMS-AIME, 1964, vol.230, p.1025.
19. J.S. Kirkaldy; Can. J.Phys., 1958, vol.36, p.907.
20. J.B. Gilmour, G.R. Purdy and J.S. Kirkaldy; Metall. Trans., 1972, vol.3, p.1455.
21. J.B. Gilmour, G.R. Purdy and J.S. Kirkaldy; Metall. Trans., 1972, vol.3, p.3213.
22. S.K. Tewari and R.C. Sharma; Metall. Trans. A, 1985, vol.16 A, p.597.
23. R.C. Sharma; Ph.D. Thesis, Mc Master University, Hamilton, Ontario, Canada, 1976.
24. R.C. Sharma, G.R. Purdy and J.S. Kirkaldy; Metall. Trans. A, 1979, vol.10 A, p.1129.
25. N.Ridley; Heat Treatment'76, The Metals Society, London, 1976, p.201.
26. N.A. Razik, G.W. Lorimer and N.Ridley; Acta. Metall., 1974, vol.22, p.1249.
27. G.R. Speich, V.A. Demarest and Q.Miller; Metall. Trans. A, 1981, vol.12 A, p.1419.
28. L.F. Porter and D.S. Dobkovski; Mascow, Metallurgiya, 1973, p.135.
29. I.N. Kidin, Mascow, Metallurgiya, 1969, p.376.
30. S.S.D'Yachenko, A.A. Movlyan, and A.I. Polyanichka; Steel in the USSR, 1987, vol.17, p.433.
31. Ye.V. Konopleva, V.M. Bayazitov, R.I. Entin and O.V. Abramov; Phys.Met. Metall., 1986, vol.61, p.104.
32. S.F. Zabelin, A.S. Tekhnov & K.S.V. Zemskii; Fiz. Khim. Orab.Meta., 1982, p.115.

33. Yu.A. Bashnin, L.A. Lisiskaya & K.C.M. Somonov; Metalloved Term. Orab. Met., 1986, vol.8, p.28.
34. G.B. Bokarov and D.T. Bukkov; Met Lenin, 1979, vol.12, p.19.
35. G.G. Sopockkin, S.I. Rirkin, V.I. Kozlor and Ya.V. Soblov; Energo Mashinosttochnic, 1981. vol.3, p.29.
36. J.S. Kirkaldy and G.R. Purdy; Can. J.Phys., 1962, vol.40, p.208.
37. A.A. Baranov; Kiev Naukova Dumka, 1974, p.231.
38. Y.M. Khlestov; Phys.Met. Metalloved, 1979, vol.47, p.998.
39. S.S.D'Yachenko; Steel in the USSR, 1972, vol.2, p.232.